HEAT TRANSFER VIA DROPWISE CONDENSATION ON HYDROPHOBIC MICROSTRUCTURED SURFACES

by

Karlen E. Ruleman

Submitted to the Department of Mechanical Engineering in partial
fulfillment of the requirements for the Degree of
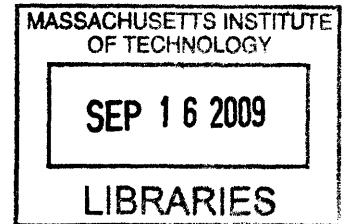
Bachelor of Science

at the

Massachusetts Institute of Technology

June 2009
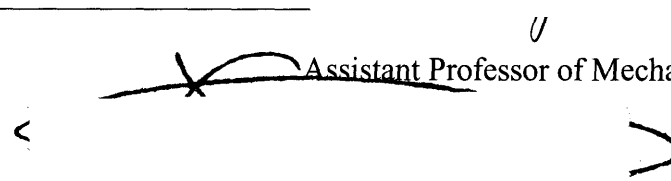
Signature of Author: _____

Karlen Ruleman
Department of Mechanical Engineering
May 8, 2009

Certified by: _____

Evelyn N. Wang
Assistant Professor of Mechanical Engineering
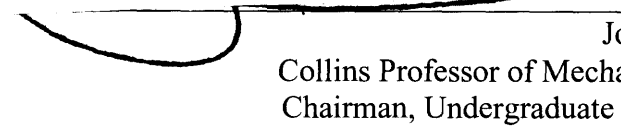Thesis Supervisor

Accepted by: _____

John H. Lienhard V
Collins Professor of Mechanical Engineering
Chairman, Undergraduate Thesis Committee

HEAT TRANSFER VIA DROPWISE CONDENSATION ON HYDROPHOBIC MICROSTRUCTURED SURFACES

by

Karlen E. Ruleman

Submitted to the Department of Mechanical Engineering on May
22, 2009, in partial fulfillment of the requirements for the Degree
of Bachelor of Science

Abstract

Dropwise condensation has the potential to greatly increase heat transfer rates. Heat transfer coefficients by dropwise condensation and film condensation on microstructured silicon chips were compared. Heat transfer coefficients are found to be seventy percent higher in the hydrophobic, dropwise condensation case relative to the hydrophilic, film condensation case. With this increased heat transfer coefficient, dropwise condensation using microstructures could improve many heat exchange applications, particularly electronics cooling.

Thesis Supervisor: Evelyn N. Wang

Title: Professor of Mechanical Engineering

Biographical Note

Karlen Ruleman is a graduate of Houston High School in Germantown, Tennessee. She will earn her Bachelor of Science in Mechanical Engineering with minors in Management and Political Science from MIT in June 2009.

Acknowledgements

I am grateful for the invaluable support and encouragement I have received from my advisor, Professor Wang, and graduate students Xiao Rong and Kuang-Han (Hank) Chu, as well as the rest of the Device Research Lab, who helped me learn rather than simply write a thesis. Many thanks also go to Dr. Barbara Hughey for her helpful advice and spare parts on several occasions.

Thanks to my parents for getting me this far, and to my professors at MIT for getting me the rest of the way.

Table of Contents

List of Figures

List of Tables

Introduction

Dropwise condensation has many applications for surfaces ranging from self-cleaning, anti-fog, anti-corrosion, and heat transfer improvements. As a specific example, heat transfer improvements associated with dropwise condensation could benefit the development of heat pipes for use in electronics cooling. However, dropwise condensation in industrial applications is very difficult to maintain, since it requires the use of surface coatings such as waxes or oils, which are worn away over time.

With a combination of nanostructures and surface coatings, the natural surface roughness of the lotus leaf can be mimicked to create superhydrophobic surfaces. In this thesis, I examine the heat transfer characteristics of microstructure dropwise condensation in comparison with film condensation.

Background

Dropwise Condensation

Dropwise condensation may be contrasted with the more common form of surface condensation, known as film condensation as shown in Figure 1. In film condensation, a liquid film covers the entire surface and acts as a thermal insulator which reduces the heat transfer rate. In dropwise condensation, the liquid coalesces as drops and rolls off the surface which allows the vapor to be in contact with the transfer surface.. The thermal resistance between vapor and surface is minimized to increase the heat transfer rate and heat transfer coefficient which can be more than an order of magnitude greater than heat transfer coefficients in film condensation (Incropera, et al. 2007).
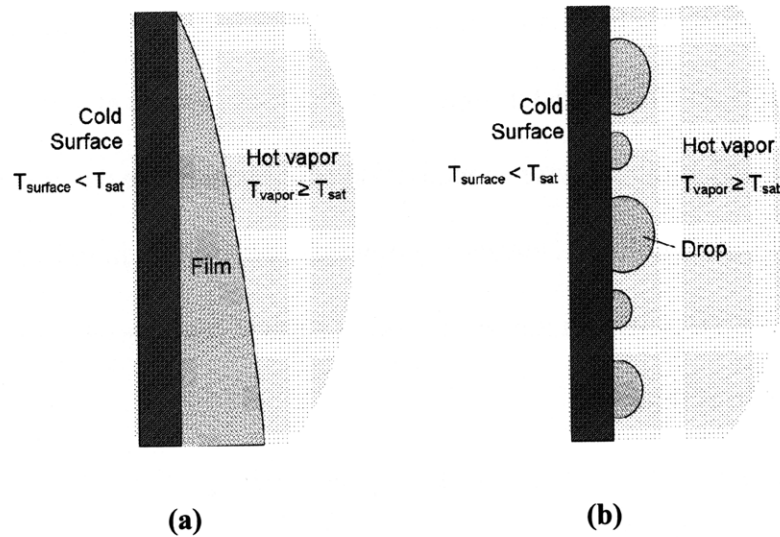
Figure 1. Modes of surface condensation.

(a) In film condensation the liquid forms an insulating layer which decreases heat transfer rates. (b) Dropwise condensation allows droplets to roll off the surface (Incropera, et al. 2007).

Dropwise condensation is currently very difficult to maintain for sustained operations. In industrial applications, heat exchangers are coated with surface coatings that inhibit wetting such as silicones, Teflon, and an assortment of waxes and fatty acids. However, these coatings gradually lose their effectiveness due to oxidation, fouling, or outright removal, leading to film condensation (Incropera, et al. 2007). Therefore, exploration into new methods of achieving dropwise condensation is merited.

Hydrophobicity

Hydrophobicity, or the ability of a surface to repel water, is characterized by its contact angle—the included angle that water droplets form on its surface. The contact angle of the hydrophobic samples used in this experiment was about 130 degrees as shown in Figure 2. The surfaces were originally manufactured to be superhydrophobic (contact angle greater than 150 degrees), but repeated testing degraded them into the hydrophobic range.
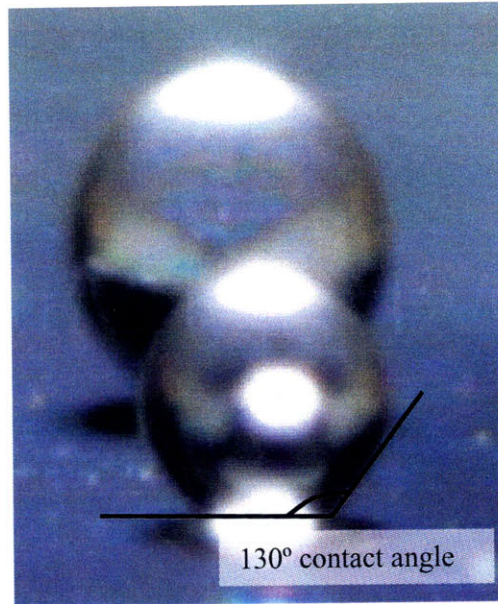
Figure 2. Contact angle.

This contact angle was 130°. After several runs, the surface
degrades and has lost its superhydrophobicity.

Fabrication of Chips

To obtain this hydrophobicity, silicon chips with microstructure features were used to
study dropwise condensation. Silicon chips may be tuned to be either superhydrophobic or
superhydrophilic depending on surface chemistry.

The process of fabricating the necessary microstructures involves several steps. First, a
photoresist coating is spun onto a silicon wafer. This makes the surface reactive to UV light.
Next, a mask, or stencil, is prepared with the desired features laid out. The spacing and diameter
of the microstructures is specified in this step. In the photolithography step, the mask is laid on
top of the wafer and exposed to UV light in the aligner. The wafer is then "developed" by
washing away material in the exposed area. Finally, the wafer undergoes deep reactive ion
etching (DRIE). The area with photoresist is protected but the remaining area is etched and
creates micron-sized pillars.

As seen in Figure 3, the microstructures used in this experiment consisted of silicon pillars of diameter 3 microns and spacing 3-5 microns. The chips have an area of 20 mm^2.
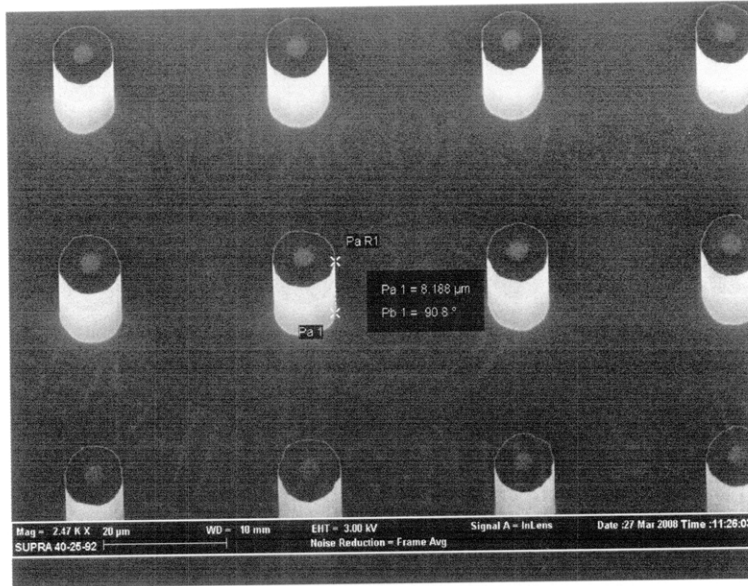
Figure 3. Microscopic image of pillars.

Scanning electron micrograph of the micropillars on a silicon substrate. The pillars are approximately 3 microns in diameter and 3-5 microns apart.

Theory

Newton's Law of Cooling

Condensation occurs when the temperature of a fluid drops below its saturation point. The fluid then comes out of the vapor phase and enters the liquid phase, losing its latent heat of vaporization during the process. Condensation most often occurs on a physical surface, through which this latent heat is transferred. The condensation rate is proportional to the heat transfer rate through this surface.

The heat flux through an area is proportional to the difference between surface and fluid temperatures, a relationship described by Newton's Law of Cooling (1),

$$\ddot{q} = h\Delta T \tag{1}$$

10

where $\ddot{q}$ is the heat flux, h is the heat transfer coefficient, and ΔT is the difference in surface and fluid temperatures. The heat transfer coefficient depends on the boundary layer, which is affected by surface geometry, the nature of the fluid motion, and an assortment of fluid thermodynamic and transport properties (Incropera, et al. 2007). In this experiment, I investigated the effect of surface properties on heat transfer coefficients.

Experimental Parameters

The heat flux is applied across the thickness of the chip. Newton's Law of Cooling, Equation (1), in this context becomes the following equation (2):

$$\ddot{q} = h\Delta T = h_{condensation}(T_{vapor} - T_{chip}) \tag{2}$$

where $\ddot{q}$ is the convective heat flux, h is the condensation heat transfer coefficient, T_{vapor} is the temperature of the vapor surrounding the chip, and T_{chip} is the surface temperature of the chip.

Solving for the variable of interest, we find the condensation heat transfer coefficient as follows as:

$$h = \frac{\ddot{q}}{(T_{vapor} - T_{chip})} \tag{3}$$

Thus, three variables must be measured in this experiment: heat flux, temperature of the vapor, and temperature of the chip.

Methods

Experimental Setup

Vapor is introduced to a sample silicon chip as shown in Figure 4. This steam elevates the relative humidity in order to promote condensation. Steam was supplied by a Tobi brand steam cleaner, after initial attempts to produce enough steam by boiling water. Care was taken to

insulate the electronics from the vapor, but saturation of electrical signals due to vapor was an

ongoing problem. The steam outlet was removed between experiments while the setup was

dried, and then replaced by aligning with guides. Chips were heated dry between runs. The

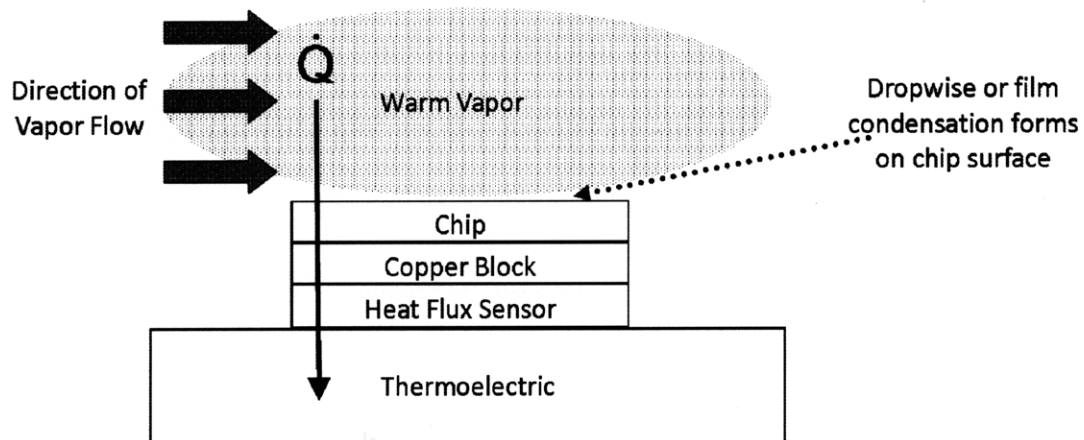experiment was run for about fifty seconds, as the temperatures stabilized in thirty seconds.

Figure 4. Schematic of experimental setup.
Warm vapor is applied to the chip as the thermoelectric removes
the thermal energy. Condensation forms on the chip surface from
this increased relative humidity and heat transfer, $\dot{Q}$.

The apparatus underneath the chip aided in the measurement and to conduct heat away

from the surface. The copper block, shown in Figure 4, housed four thermocouples using

Omegabond 101 thermal epoxy. The heat flux sensor was placed directly under the block. The

active refrigeration thermoelectric at the bottom of the stack included a thermoelectric

refrigerator, a copper sink, and the laboratory optical table. The thermoelectric refrigerator

operated at a power of 12 W and unknown efficiency. Omegatherm thermal grease between

each layer (and thermal epoxy between the copper block and thermocouples) was used to ensure

that all parts had minimal thermal resistance. Thus, neglecting the thermal grease, thermal

energy transferred through a series of resistances, shown in Figure 5. The surface area associated
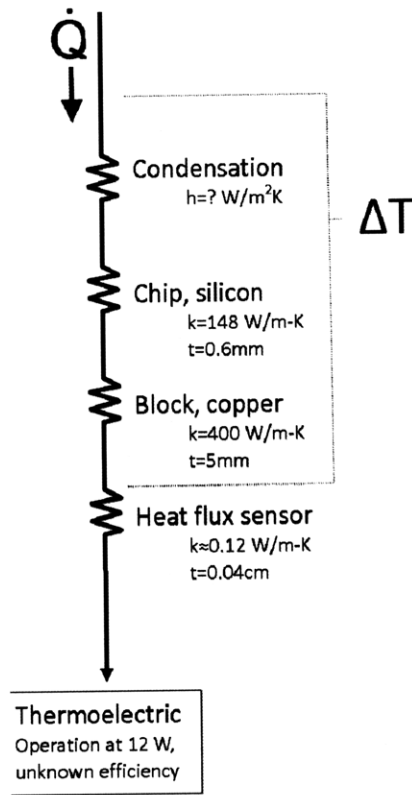
with all of these resistances is 4 cm^2.

Figure 5. Thermal resistances involved in experimental setup.

The total thermal resistance is associated with condensation, the silicon, chip, copper block, heat flux sensor, and thermal grease (not shown). The temperature difference was measured between the air slightly above the chip and the copper block across the resistances indicated.

Sensors

To measure the necessary variables (heat flux, temperature of the vapor, and temperature

of the chip), a variety of sensors are needed, listed in Table 1. The location of these sensors is

shown in Figure 6. National Instruments DAQ card and I/O controller SCB-68 were used as the

data acquisition hardware. The 16-input DAQ card limited the setup to seven sensors, using a

differential configuration.

Table 1. Table of sensors.

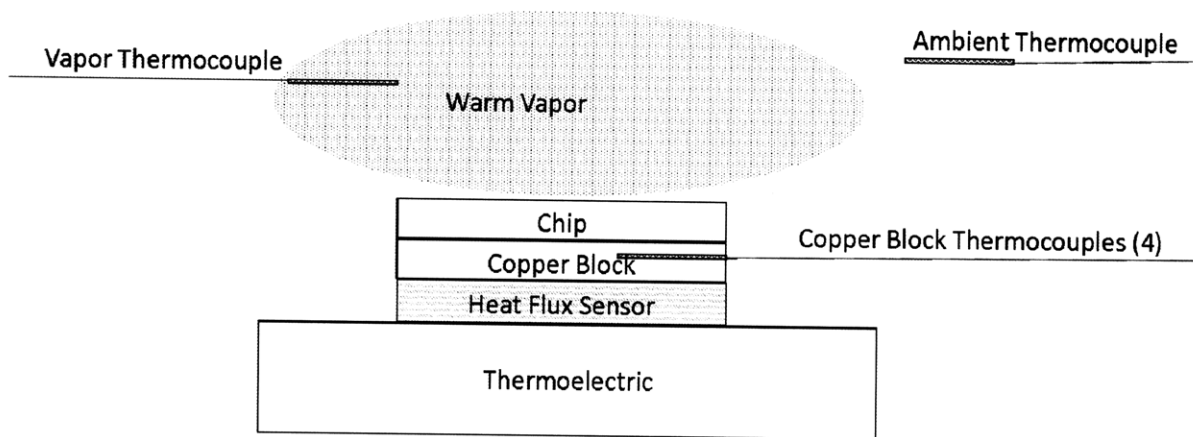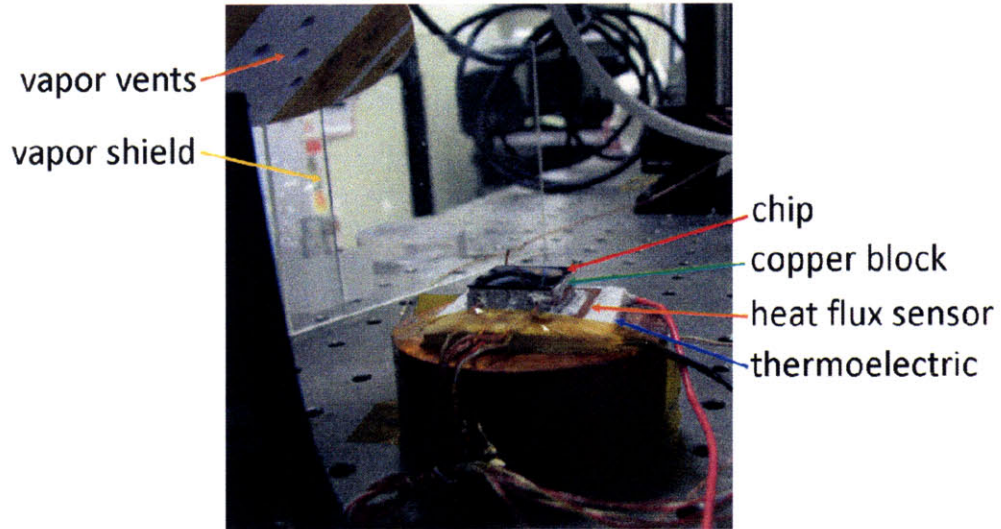| Sensor	Measurement
Cold Junction Compensation (CJC)	Reference temperature for other thermocouples
Thermocouple 1	Temperature spatial variation of chip via copper block
Thermocouple 2	
Thermocouple 3	
Thermocouple 4	
Thermocouple 5	Ambient temperature
Thermocouple 6	Vapor temperature
Heat Flux Sensor	Flux over chip area

Figure 6. Location of sensors.

Six thermocouples are placed to measure necessary temperatures and the heat flux sensor is placed between the chip and the heat sink.

The cold junction compensation, or CJC, was used as a reference point for all thermocouples. Thermocouples measure temperature via the *Seebeck effect*—when two dissimilar metal wires touch, an open-circuit voltage is formed across the ends. This voltage can be related to temperature (through an eighth-order equation). Since thermocouples measure the temperature difference between two points, the temperature at their voltage leads needed to be measured by the CJC sensor. The CJC sensor was built into the SCB-68.

Figure 7 shows the layout of the experimental setup.

(a)
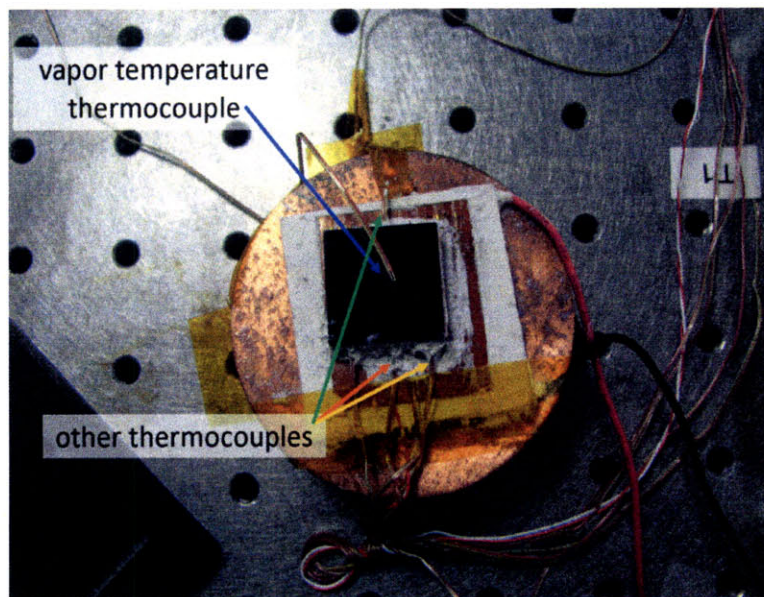
(b)

Figure 7. Images of experimental setup.

Thermocouples 1-4 embedded in the copper block measured T_{chip}, the temperature of the silicon chip. The four K-type thermocouples allowed for measurement of the spatial variation in the chip in two dimensions. This was especially important because the application of the steam vapor was asymmetrical. The layout of the thermocouples is shown Figure 8. These thermocouples were averaged to find the average temperature of the chip.
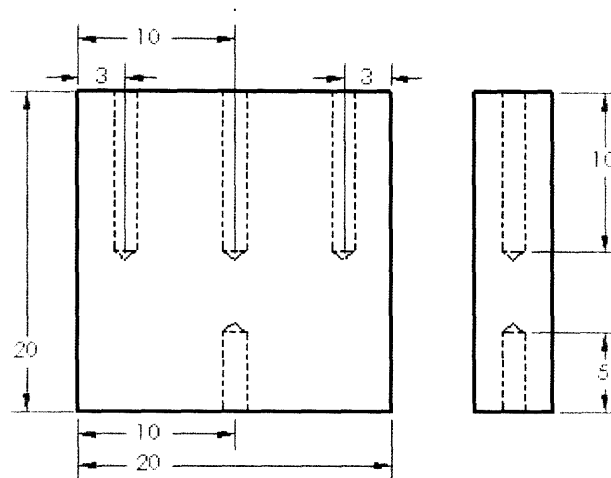
Figure 8. Interior of copper block.

Holes were drilled for the insertion of thermocouples to measure the
spatial variation in temperature of the chip. All dimensions are in
millimeters.

Thermocouple 5 measured the ambient air temperature for consistency among experiment

runs. Thermocouple 6 measured the vapor temperature and was placed 7mm above the center of

the chip.

The final sensor was an Omega HFS-4 heat flux sensor. This used a multi-junction

thermopile to measure heat flux through its surface area, which, like the silicon chip, measured 2

cm by 2 cm. The voltage output was proportional to heat flux (2.06 μV per W/m^2, $\pm$10%).

Results

Heat Transfer Coefficients

Data was obtained for two cases: film condensation on a hydrophilic chip and dropwise

condensation on a hydrophobic chip. An unstructured silicon surface was also tested, but

dropwise condensation was observed rather than film condensation due to oils acquired in

handling. All chips were in the horizontal position, so water collected continuously. The

hydrophilic case was especially sensitive to handling and had to be plasma-cleaned to obtain film

condensation. The hydrophobic chip was manufactured to be superhydrophobic, but lost some
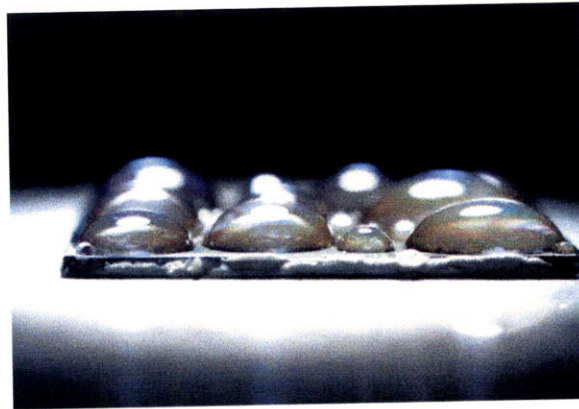
of its effectiveness in repeated testing, so it is considered here to be only hydrophobic. The hydrophilic chip immediately developed film condensation across the entire surface of the chip, as shown in Figure 9 (a). The hydrophobic chip accumulated drops which increased in size as the experiment run progressed, shown in Figure 9 (b) and (c).

(a)

(b)

(c)

Figure 9. (a) Film condensation on a hydrophilic chip.
(b) and (c) Two views of dropwise condensation on hydrophobic chip.

Film condensation covers the entire chip surface immediately. Dropwise condensation begins as very tiny drops which coalesce into the up to 7 mm diameter drops shown here.

An instantaneous heat transfer coefficient was calculated from data. A sample hydrophilic run is shown in Figure 10. Note that the heat transfer coefficient is plotted with

respect to the right vertical axis and the vapor temperature with respect to the left vertical axis. From this graph, we can see that the rise time for the heat transfer coefficient is much greater than that of vapor temperature. Although the vapor temperature remains constant, the heat transfer coefficient continues to rise, taking about thirty seconds to reach a semi-equilibrium state. Spikes in heat transfer coefficient correspond with drops in vapor temperature and are a result of intermittent steam quality.
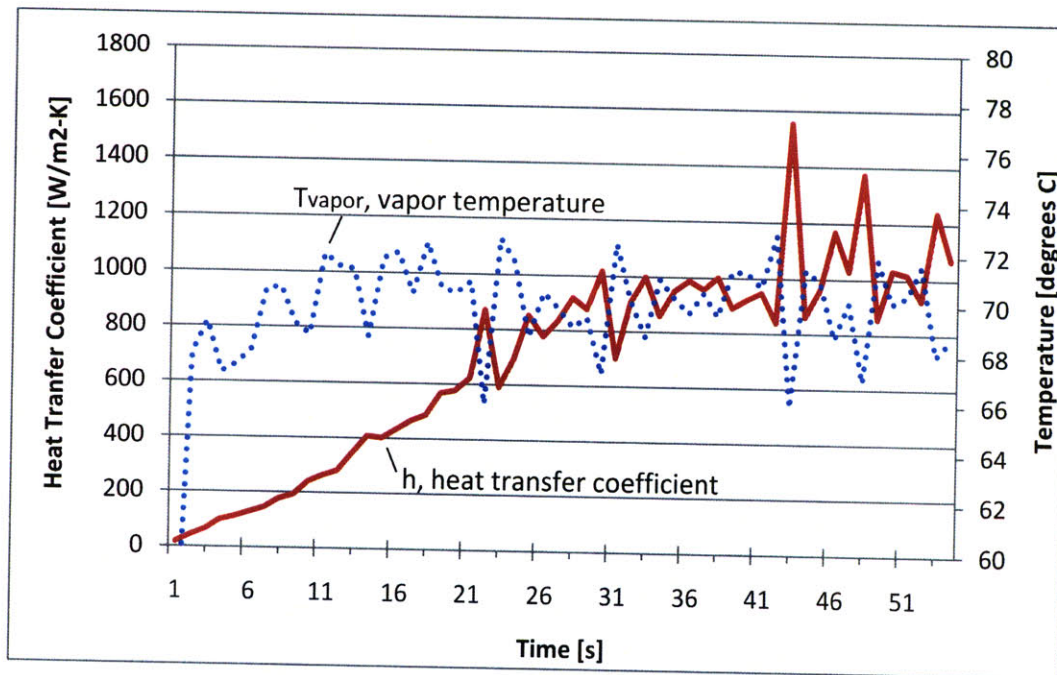

Figure 10. Variation in heat transfer coefficient over time in a hydrophilic example.

Note that the heat transfer coefficient is plotted on the left vertical axis and the vapor temperature is plotted on the right vertical axis. Note that the temperature scale does not start at 0. The rise time for the heat transfer coefficient is much greater than that of vapor temperature, but the heat transfer coefficient stabilizes at about 30 seconds. Spikes in heat transfer coefficient correspond with drops in vapor temperature and are a result of high sensitivity to the vapor temperature sensor and intermittent steam quality.

Heat transfer coefficients were calculated at this equilibrium state for four runs. The results are shown in Table 2. The hydrophobic chips exhibited steady-state overall condensation

heat transfer coefficients of 1400 W/m²-K and 1200 W/m²-K. Hydrophilic chips had heat transfer coefficients of 770 W/m²-K and 760 W/m²-K. In this case, the heat fluxes across both cases were about equal because the chip was in contact with a constant flux surface, the thermoelectric, rather than an isothermal surface, which would have given higher fluxes to the hydrophobic case.

Table 2. Heat transfer coefficient results for hydrophobic and hydrophilic cases.

measurement	variable	unit	hydrophobic			hydrophilic	
			phobic 1	phobic 2		philic 1	philic 2
heat flux	$\ddot{q}$	[V]	0.026	0.030		0.030	0.022
heat flux	$\ddot{q}$	[W/m²]	12600	14600		14600	11000
vapor temp	T_{vapor}	[deg C]	70	72		74	70
chip temp	T_{chip}	[deg C]	61	60		55	56
temp difference	ΔT	[deg C]	9	12		19	14
heat transfer coefficient	h	[W/m²-K]	1400	1200		770	760

The hydrophobic heat transfer coefficients are significantly higher (70% higher, on average) than the hydrophilic heat transfer coefficients. Therefore, dropwise condensation does have higher heat transfer rates than film condensation, as expected.

Possible Improvements

The improvement in the heat transfer coefficients is not as large as those found in the literature. This is most likely due to the degradation of the chips over many experiment runs. The superhydrophobic and hydrophilic conditions are difficult to maintain as the surface must remain entirely free of contaminants.

The chips did not exhibit a lot of spatial variation in temperature—thermocouples 1-4 were within two degrees of one another. However, the vapor temperature measurement was

quite sensitive to location, and the entire heat transfer coefficient calculation was very sensitive

to this measurement. Care was taken not to disturb the vapor temperature thermocouple during

changing of chips, but future experiments should fix this sensor better and include multiple

sensors to measure vapor temperature.

One other possible source of error was the quality of steam from the steam source. Vapor

output was observed to be intermittent in mass flow rate. Experiments were taken over periods

with relatively constant vapor output, but this limited the run time to tens of seconds. With a

more consistent steam source, longer datasets could be taken for a more reliable result. In an

alternative experimental design, a more powerful thermoelectric could lower the temperature of

the chip below the dew point, causing condensation to form from the ambient air with no steam

source required. The thermoelectric used was capable of this, but only after long periods of time.

Additionally, condensation should be examined with the chips in the vertical position.

This would allow for a better steady-state condition as the water would both collect and roll off,

better approximating heat exchangers in industrial applications.

Conclusion

The heat transfer coefficient was found to be 1300 W/m^2-K, on average, for the

hydrophobic case, and 770 W/m^2-K, on average, for the hydrophilic case. Thus, as expected, the

hydrophobic coefficient was larger (by 70%) than the hydrophilic coefficient. This reflects the

fact that dropwise condensation is a more effective heat transfer mechanism than film

condensation. For a discussion on heat transfer coefficients of similar microstructured silicon

chips based on an evaporation experiment, see Xiao (2009).

The literature indicates that dropwise condensation can achieve an order of magnitude

improvement on film condensation. Our findings fall short of the theoretical maximum for two

main reasons. First, the chips used had lost their superhydrophobicity due to surface contamination and were merely hydrophobic. The contact angles apparent in Figure 9 are much less than 130 degrees as calculated previously and in fact appear to be less than 90 degrees. Increased hydrophobicity would increase heat transfer coefficients. Second, the experiment was performed with the chips in the horizontal position, which allowed water to collect on the surface in both cases. However, with chips placed in the vertical position, water would roll off. This effect would be greater in the hydrophobic case since droplets would wet the surface less. This would greatly reduce the resistance effect of the liquid water, and heat transfer coefficients would be increased.

Appendix 1 – Bibliography

AI-Baroudi, H. M., & Klein, A. C. (1995). Experimental Simulations and Heat Transfer Parameter Measurements of Film Condensation on a Rotating Flat Plate. *Experimental Thermal and Fluid Science* (10), 124-135.

Cassie, A. B., & Baxter, S. (1944). Wettability of Porous Surfaces. *Transactions of the Faraday Society* , 546-551.

Chen, C., Cai, Q., & Tsai, C. e. (2007). Dropwise condensation on superhydrophobic surfaces with two-tier roughness. *Applied Physics Letters , 90* (17), 173108.

Incropera, F. P., Dewitt, D. P., Bergman, T. L., & Lavine, A. S. (2007). *Introduction to Heat Transfer* (Fifth Edition ed.). Hoboken, NJ: John Wiley & Sons.

Wenzel, R. N. (1936). Resistance of Solid Surfaces to Wetting by Water. *Industrial & Engineering Chemistry , 28* (8), 988-994.

Xiao, Rong. *Nanoengineered Surfaces for Advanced Thermal Management.* Master's Thesis, forthcoming, Massachusetts Institute of Technology, 2009.

Zheng, Y., Han, D., Zhai, J., & Jiang, L. (2008). In situ investigation on dynamic suspending of microdroplet on lotus leaf and gradient of wettable micro- and nanostructure from water condensation. *Applied Physics Letters , 92* (8), 084106.

Appendix 2 – LabVIEW Code

LabVIEW 8.6 was used as the data acquisition software. The following figures show the front panel user interface and the block diagram code.
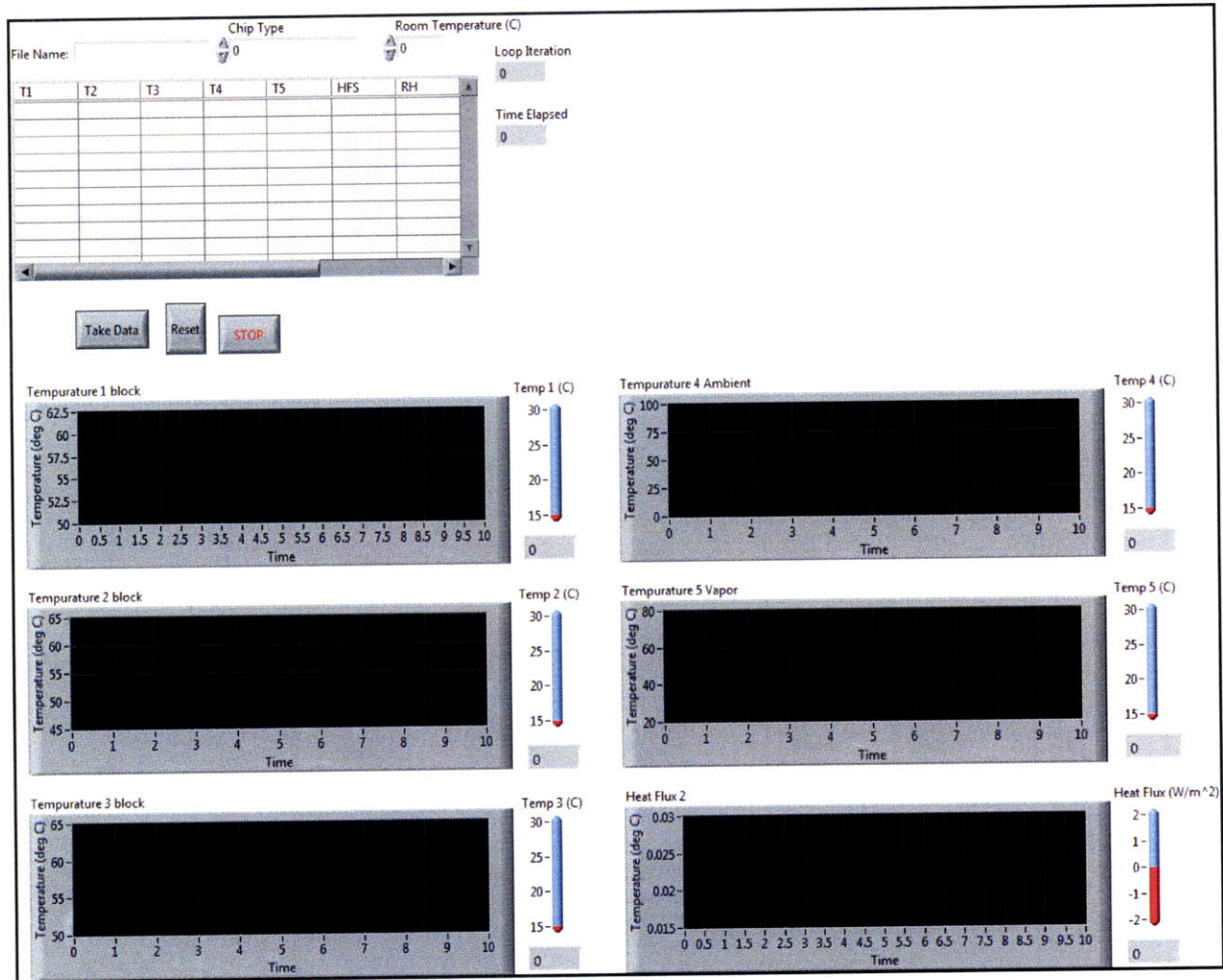

Figure 11. Front panel user interface.

The user interface included fields for inputting chip type and room temperature, a display table of accumulating data averages, and charts which showed the last ten seconds of temperature and heat flux data.
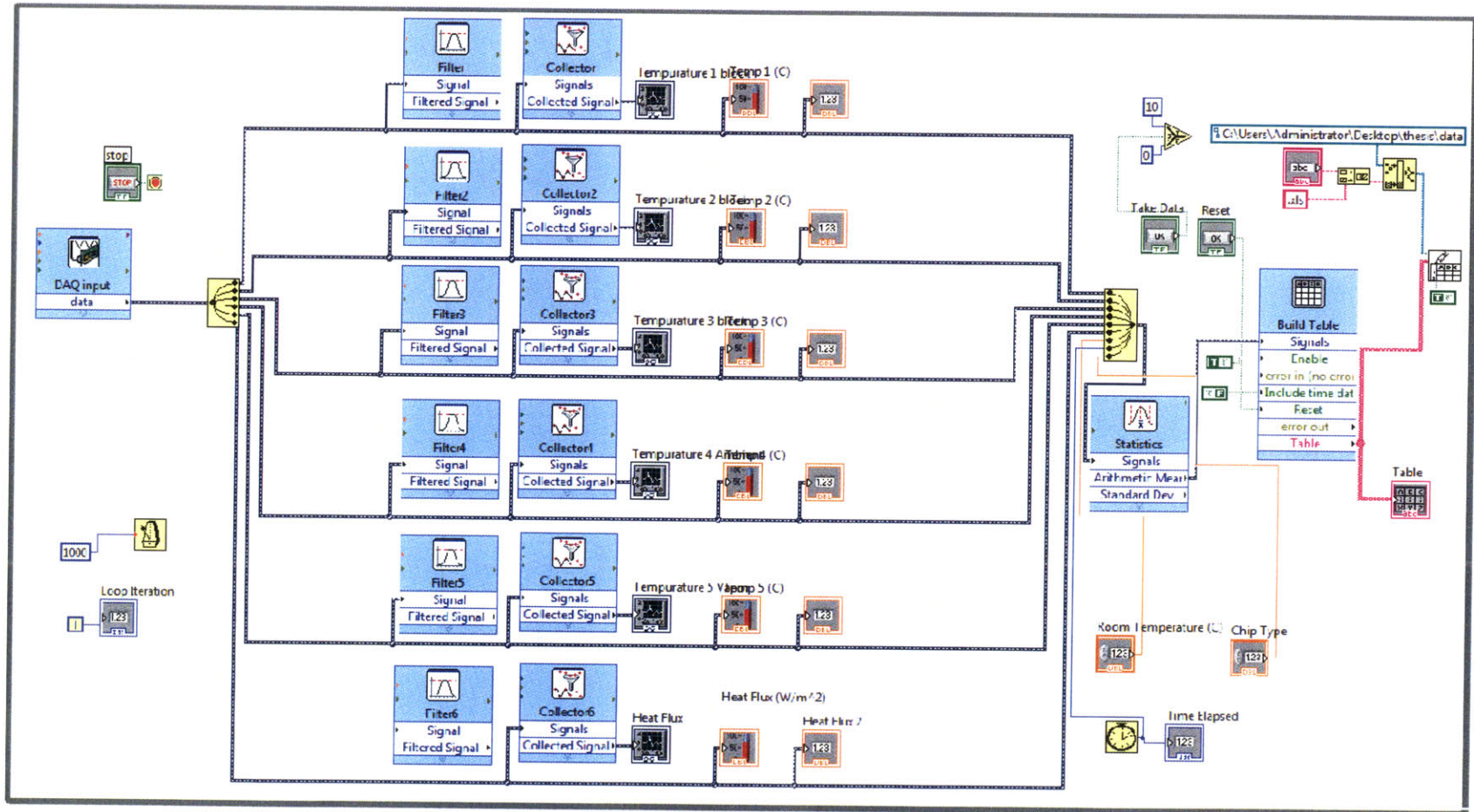
Figure 12. Block diagram of LabVIEW code.

Data is input from the DAQ card and sent to front panel displays. Data is averaged over 0.1 second intervals once every second and compiled into a generated Microsoft Excel file.